# A SIMS and TEM investigation of the microstructure of wear-resistant ductile cast iron

Nathalie Valle, Mayerling Martinez Celis, Jacques Lacaze, Ingólfur Örn Thorbjornsson, Birgir Johannesson, Jon Thor Thorgrimsson

# A SIMS and TEM investigation of the microstructure of wear-resistant ductile cast iron

N. Valle,[a]* M. Martinez Celis,[a] J. Lacaze,[b] I. O. Thorbjornsson,[c] B. Johannesson[c] and J. T. Thorgrimsson[d]

**The benefit of the presence of Cr containing inserts inside ductile iron on the tribological properties of these materials has been recently demonstrated. In order to understand these improved properties, a secondary ion mass spectrometry (SIMS) and transmission electron microscopy investigation of these wear-resistant ductile cast irons has been performed. The results indicate that the principal change in the microstructure induced by inserts occurs in the inserts and in their surroundings where the formation of carbides with different sizes and compositions is observed: $M_3C$, $M_7C_3$ and $M_{23}C_6$ (M stands for Fe and/or Cr). These are not pure binary carbides since among the different elements studied by SIMS, Cr, Fe, Mn and, to a lesser extent, Ni are soluble in these carbides**. Copyright © 2012 John Wiley & Sons, Ltd.

**Keywords:** microstructure; ductile cast iron; chromium carbides; TEM; nano-analysis SIMS

## Introduction

Ductile irons are essentially ternary Fe–C–Si alloys in which the concentrations of carbon and silicon vary typically in the range of 3.5–3.9% and 1.8–2.8%, respectively. In ductile iron, graphite is in the form of spherical nodules thanks to the addition to the melt of tiny amounts of spheroidising elements such as magnesium. These nodules provide an enhanced ductility to the material. The majority of the castings produced with nodular cast irons have a pearlitic, a ferritic or a ferritic–pearlitic matrix in the as-cast state.[1,2]

Ductile irons are used in demanding applications for which the load and wear are usually localized at the surface of parts. In order to improve their wear resistance, a successful surface hardening can be obtained by the introduction of chromium containing steel inserts in the mould of parts to be cast with ductile iron.[3] The basic idea, already mentioned by Qian *et al.*,[4] is to form hard carbides by using stainless steel inserts as a source of chromium and the ductile iron as a source of carbon. The tribological properties of reinforced ductile irons can be further improved when subjected to austempering treatment.[5]

In order to understand this local reinforcement, the microstructure, the composition of carbides and the distribution of elements in the wear-resistant ductile iron were characterized using transmission electron microscopy (TEM) and secondary ion mass spectrometry (SIMS).

## Materials and methods

### Materials

The reinforced ductile iron studied has been elaborated by following the steps described in the patented process detailed in reference [[3], see also[6]]. The inserts were made of stainless steel, i.e. Fe–Ni–Cr alloy containing about 16–20 wt% Cr, 8 wt% Ni and small amounts of manganese and silicon.

Cylinder-shaped inserts were appropriately located in the mould cavity where the improved wear resistance is required for the final part. Their thickness and size were, respectively, in the ranges of 1–2 mm and 5–10 cm. The melt used in the present study is an unalloyed standard nodular cast iron (C: 3.7–3.9 wt.%, Si: 2.7–2.8 wt.%, Mn: 0.12–0.16 wt. %, Mg: 0.03 wt%, Cu: 276–426 ppm, Ni: 268–345 ppm, P: 219–265 ppm, S: 109–110 ppm, Mo $<$ 10 ppm). The casting conditions were adapted to guarantee a partial dissolution of the inserts before solidification of the cast iron. A sample machined out from the casting has been analyzed in its as-cast state and another one after austempering. The austempering treatment consists of a two-stage process: a heating to and holding at 900 °C for 60 min followed by a quench to 300 °C and holding at that temperature for 75 min before air-cooling.

### Analytical techniques

SIMS experiments were carried out with a CAMECA NanoSIMS 50 instrument to investigate chromium carbides from the core of the insert to the bulk of the ductile iron. The coaxial optics of the NanoSIMS imposes an opposite polarity for primary ions ($Cs^+$ or $O^-$ from the ion source) and secondary ions (from the

* *Correspondence to: N. Valle, Centre de Recherche Public - Gabriel Lippmann, 41, rue du Brill, L-4422 Belvaux, Luxembourg. E-mail: valle@lippmann.lu*

a *Centre de Recherche Public - Gabriel Lippmann, 41, rue du Brill, L-4422 Belvaux, Luxembourg*

b *CIRIMAT, Université de Toulouse, BP 44362, 31030 Toulouse cedex 4, France*

c *Innovation Center Iceland, Keldnaholt, 112, Reykjavik, Iceland*

d *Malmsteypa Thorgrims Jonssonar, Midhraun 6, 210, Gardabaer, Iceland*

sample). While the use of $Cs^+$ primary ion favours the emission of carbon as a negative ion, the use of a $O^-$ primary ion allows to enhance ion emission of positive chromium ion $Cr^+$. A compromise was found by studying the chromium carbides through the measurements of the cluster $CrC^-$ with a caesium primary source at an energy of 16 keV. The different $CrC^-$ images, with a size of 256×256 pixels, were acquired simultaneously to those of $C^-$ and $Si^-$ thanks to a multicollection system by using a focused $Cs^+$ primary ion beam (few pA, probe size ≈200 nm) scanned across an area of a few tens of micrometers in size. A presputtering of the surface was performed before any measurement in order to minimize the surface contamination (mainly carbon and oxygen). The acquisition times per image were around 5–10 min. The mass resolution defined as the ratio M/ΔM was around 3000.

To complement the investigation of chromium carbides, the imaging of positive ions ($Mn^+$, $Cr^+$ and $Ni^+$) was performed on a modified CAMECA IMS 6f equipped with a gallium liquid metal ion gun operating at an energy of 25.5 keV. Contrary to NanoSIMS analyses, the analyses were performed in monocollection mode. They were assisted with oxygen flooding ($10^{-6}$ mbar) for a higher sensitivity. The primary beam with an intensity of around 150 pA was focused down to 500 nm. The mass resolution was around 300. The counting times for $Cr^+$, $Ni^+$ and $Mn^+$ were 20 s.

For SIMS measurements, each specimen studied contained at least one stainless steel insert. Rectangular parallelepiped-shaped samples were cut in the direction parallel to the length of the insert in order to image the distribution of carbides in the region all around the inserts. They were polished with SiC paper up to grade 1000 and then with diamond pastes (7, 3 and 1 μm) before being embedded in a Wood's alloy in a copper ring of 8 mm in diameter. The samples were then ultrasonically cleaned in alcohol.

At the same time, microstructure observations and electron diffraction for phase identification were carried out by TEM with a LEO 922 OMEGA operating at 200 kV. Thin foils were prepared by mechanical polishing disc specimens of 3 mm in diameter down to 100 μm. Then, a precision dimple grinder instrument was used to reduce the thickness of the disc down to 50 μm at the thinnest part of the dimple. For the last step of thinning, ion milling was preferred to electropolishing because of the large differences between the phases present in the sample. The angles of the two ion beams in the final stage of milling were set at 6° for best results.

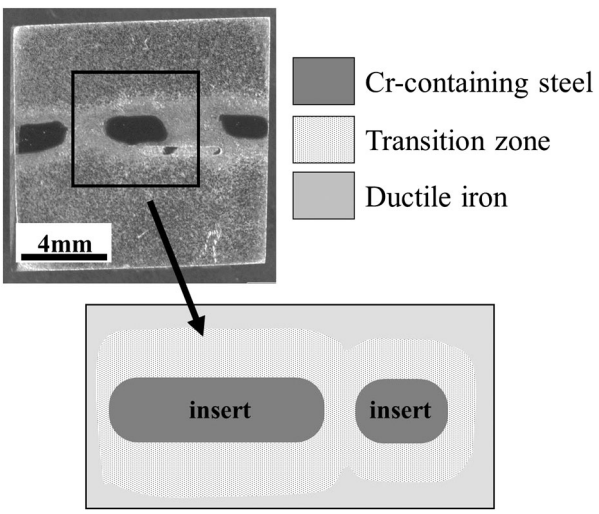


**Figure 1.** Description of the different regions of the reinforced ductile iron.

## Results

The reinforced ductile iron consists of stainless steel inserts fixed inside the cast iron as illustrated in Fig. 1. A rapid observation under optical microscope highlights three well-marked areas for each specimen: the Cr containing steel inserts, a region surrounding the inserts called the **transition zone** and further away from the inserts, the ductile iron.

During casting, the partial dissolution of the external part of the insert produces a flux of elements, mainly chromium, from

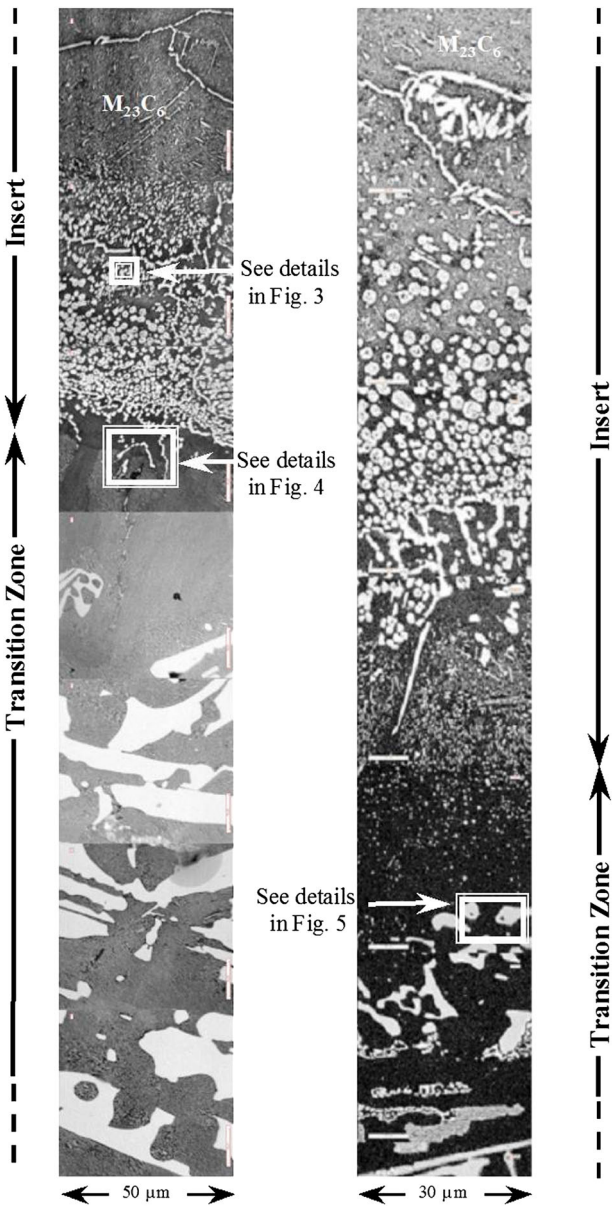


**Figure 2.** $^{12}C^{52}Cr^-$ ion images of an as-cast sample (left) and after austempering (right). White contrast represents highest intensities of the element, while black contrast represents lowest intensities.

the insert to the liquid cast iron. At the same time, carbon present in the melt diffuses in the opposite direction into the solid insert. This results in a gradual modification of the microstructure in the region surrounding the inserts.[7] The resulting transition zone is characterized by a composition and a microstructure which differ from those of the insert and the ductile iron. Depending on the casting conditions and the size of the inserts, the transition zone can extend to 2 mm.

The insert and the transition zone have been investigated by SIMS. The $CrC^-$ maps, placed end to end from the core of the insert up to a distance of about 200 μm from its border, reveal the existence of chromium carbides in different shapes and sizes (Fig. 2).

## The insert

The carbides, the most enriched in chromium, identified by TEM as $M_{23}C_6$, have been found furthest within the insert (over 80 μm) where the matrix is composed of austenite.[7] While the biggest ones are visible on the SIMS maps (fig. 2), others with 50 nm in size were only observable by TEM. Most of them are intragranular and are next to some scarce big lamellar carbides (up to 20 μm in size, top right-hand side in Fig. 2). Nearer the interface, a second type of chromium carbide appears over a region covering around 50 μm. The associated electron diffraction pattern corresponds to $M_7C_3$ carbides (Fig. 3). These precipitates are ring shaped with a uniform composition in chromium and carbon. As revealed by the SIMS maps, they also contain manganese while nickel (not shown here) and silicon are rejected in the core outside of the ring (Fig. 3). The region containing $M_7C_3$ carbides can be as thick as 50 μm with an increase of carbides density as one moves towards the border of the insert.

The formation of a third type of carbide identified as $M_3C$ (Fig. 4) takes place inside grains and at grain boundaries in the most external part of the insert, which is characterized by an important depletion of chromium content. This region can extend up to 10 μm and is adjacent to the transition zone. The interface between these two areas is clearly visible for the as-cast sample on the $C^-$ ion map where the pearlite exhibits a lamellar mixture of ferrite (grey contrast) and cementite (white contrast) whereas the $C^-$ image of the matrix that consists in martensite is much less contrasted. The transition martensite / pearlite corresponds to the interface insert / transition zone.

No significant changes in microstructure were observed in the insert after austempering treatment.

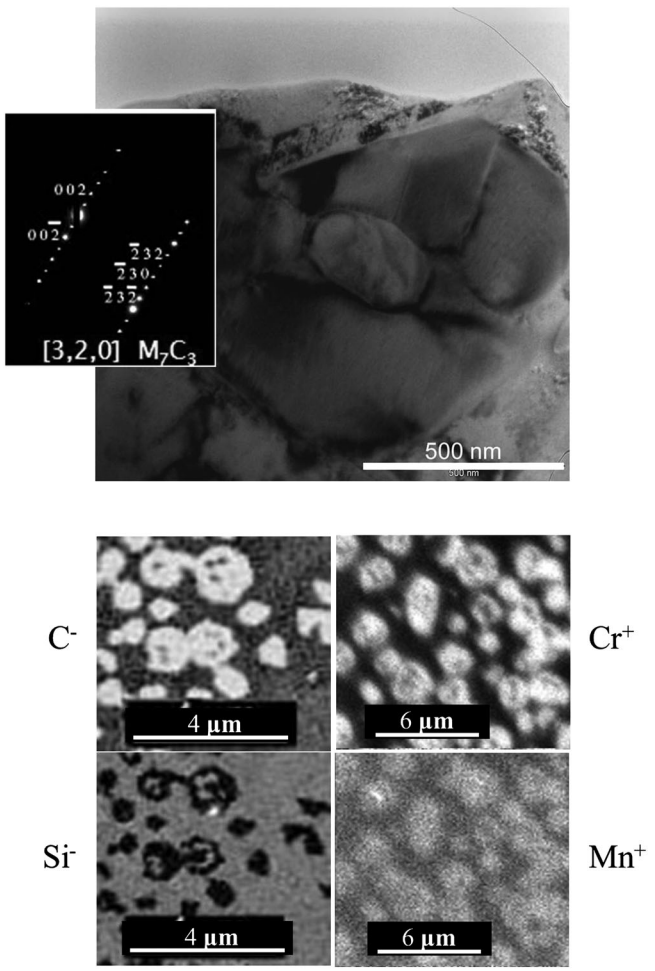


**Figure 3.** Round $M_7C_3$ carbides in the insert. At the top: TEM micrograph and diffraction pattern, zone axis [3 2 0]. At the bottom: SIMS maps of $C^-$, $Si^-$, $Cr^+$ and $Mn^+$. The images have been obtained in different areas for negative and positive mode.

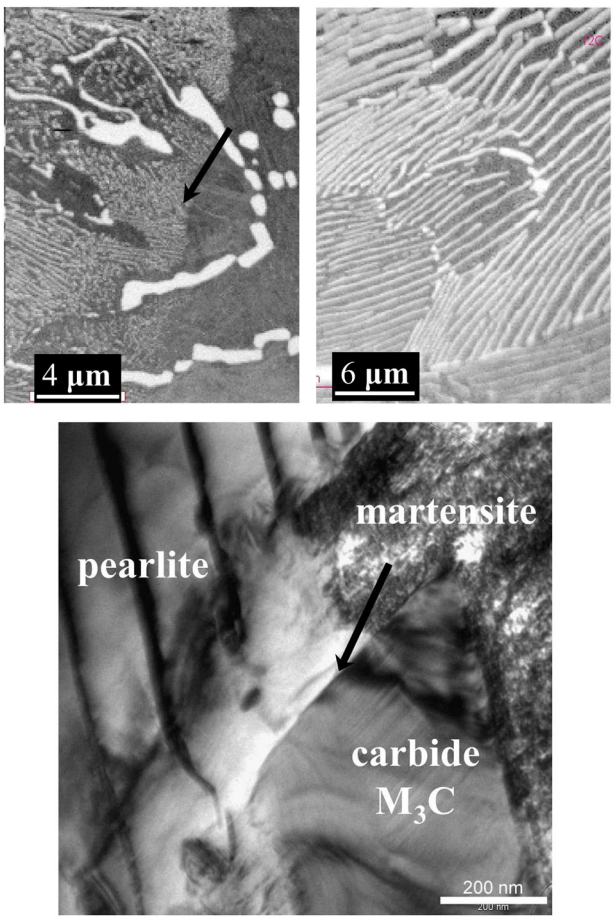


**Figure 4.** Microstructure in the transition zone, next to the insert, for the as-cast sample. At the top: $C^-$ ion maps. At the bottom: TEM micrograph. The black arrows indicate the position of the interface insert / transition zone. Pearlite, martensite and $M_3C$ carbides have been identified by TEM (the electron diffraction patterns are not shown here).

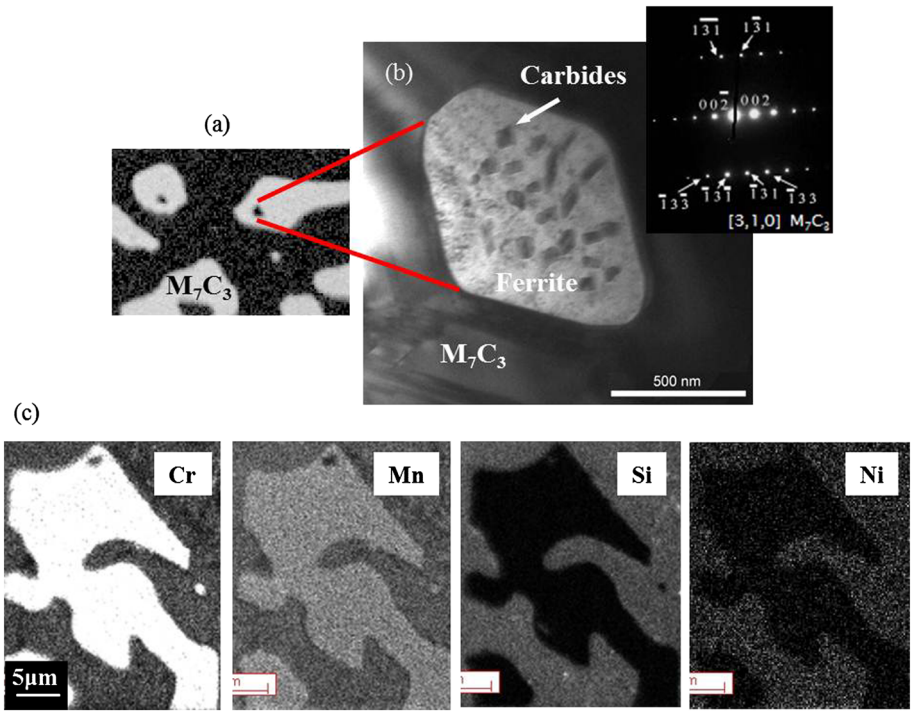


**Figure 5.** $M_7C_3$ carbides in the transition zone, next to the insert. (a) SIMS maps of $CrC^-$ (b) TEM micrograph and diffraction pattern, zone axis [310]. (c) SIMS maps of $C^+$, $Mn^+$, $Si^+$ and $Ni^+$ distribution inside $M_7C_3$ carbides.

## The transition zone

The transition zone of the as-cast sample is composed of carbides, pearlite, ferrite and graphite nodules, smaller near the insert than in the bulk of the cast iron and without the ferrite shell existing in ductile iron. The nodules density increases up to the bulk of cast iron. The proportion of the different phases graphite, carbides, pearlite and ferrite determined at a distance of 100 µm and 1300 µm from the edge of the insert change, respectively, from 2.5 to 10%; 10.9 to 1%; 86.6 to 30.8% and 0 to 58.2%. The transition zone is composed of three distinct regions. The first one, adjacent to the interface, consists of a band of pearlite whose thickness can reach up to 100 µm. Further away from the interface, the presence of two types of carbides, $M_3C$ and $M_7C_3$, has been confirmed by electron diffraction (Fig. 2, Fig. 5 and[7]). The second region of the transition zone, spreading to 80 µm, contains both types of carbides whereas only $M_3C$ is present in the third region covering the largest part of the transition zone (~1800 µm). Inside a few $M_7C_3$ precipitates, a ferrite islet (black contrast in Fig. 5-a) containing small non-identified carbides (50 nm in size, Fig. 5-b) can remain. The $M_7C_3$ carbides present a uniform composition in Cr and Mn, and they are free from Si and could contain some traces of Ni (Fig. 5).

After austempering treatment, the matrix is transformed into ausferrite, and some $M_7C_3$ type carbides are partially dissolved in the region near the inserts (bottom right side in Fig. 2).

## Conclusion

The reason for the improved wear properties of reinforced ductile cast iron[5] is found in the modification of the microstructure induced by the introduction of stainless steel inserts in the mould before casting. The local hardening is due to the formation of hard carbides in the insert and in its surroundings. Although the nano-analysis SIMS allows, thanks to the acquisition of $CrC^-$ maps, to give evidence of the presence of carbides, their identification requires electron diffraction pattern.

Three different types of carbides have been found in reinforced ductile iron: $M_3C$, $M_7C_3$, $M_{23}C_6$. They are present together in the insert, while only $M_3C$ and $M_7C_3$ coexist in the transition zone. They are not pure binary carbides since among the different elements studied by SIMS, Cr, Fe, Mn and, to a lesser extent, Ni are soluble in these carbides. The solubility of these elements depends on the type of carbide.[8,9]

### Acknowledgements

The authors wish to thank E. Lentzen, P. Grysan and B. El Adib for their helpful contribution to this work. This work was financially supported by the Fonds National de la Recherche du Luxembourg (DIWEAR project, INTER - ERA-Net MATERA programme).

## References

[1] J. R. Davis, *Cast irons*, ASM International, Materials Park, OH, **1996**.
[2] C. Labrecque, M. Gagné. Ductile iron. *Can. Metall. Quart.* **1998**, *37*(5), 343–378A.
[3] I. Ö. Thorbjörnsson, J. T. Thorgrímsson, international patent application under the PCT treaty, WO 2009/081420, **2009**.
[4] M. Qian, S. Harada, Y. Kuroshima, H. Nagayoshi, *Mater. Sci. Eng. A* **1996**, *208*, 88–92.
[5] B. Podgornik, J. Vizintin, I. Thorbjornsson, B. Johannesson, J. T. Thorgrimsson, M. Martinez Celis, N. Valle, *Wear* **2012**, *274–275*(27), 267–273.
[6] I. Thorbjörnsson, B. Jóhannesson, J. T. Thorgrimsson, *Int. J. Cast Met. Res.* **2011**, *24*(6), 333–337.
[7] M. Martinez Celis, N. Valle, J. Lacaze, I. O. Thorbjornsson, B. Johannesson, J. T. Thorgrimsson, *Int. J. Cast Met. Res.* **2011**, *24*(2), 76–82.
[8] T. Sourmail, *Mater. Sci. Technol.* **2001**, *17*, 1–14.
[9] A. F. Padilha, P. R. Rios, *ISIJ Int.* **2002**, *42*, 325–37.